Available online at www.sciencedirect.com
SCIENCE DIRECT
Dyes and Pigments 67 (2005) 139–144
DYES and PIGMENTS
www.elsevier.com/locate/dyepig

Intermolecular interactions of flavanthrone and indanthrone pigments

D. Thetford[a,*], J. Cherryman[b], A.P. Chorlton[c], R. Docherty[d]

[a]Lubrizol Ltd, Research Department, PO Box 42, Hexagon House, Blackley, Manchester M9 8ZS, UK
[b]Intertek Ltd, Research Department, PO Box 42, Hexagon House, Blackley, Manchester M9 8ZS, UK
[c]Pharmorphix Ltd, 250 Cambridge Science Park, Milton Road, Cambridge CB1 0WE, UK
[d]Pfizer Central Research, Sandwich, Kent CT13 9NJ, UK

Received 4 September 2004; received in revised form 5 November 2004; accepted 10 November 2004
Available online 21 January 2005

Abstract

Using computational chemistry techniques, the structures of flavanthrone (**1**) and indanthrone (**2**) have been re-examined. The similarity in the packing motifs of indanthrone and flavanthrone has been studied and the important intermolecular interactions have been determined. The role of weak hydrogen bonds of the type C–H:::::O in the formation of the three dimensional structures have been clarified.

Keywords: Molecular modelling; Pigments; Lattice energy; Intermolecular interactions

1. Introduction

In recent years, the study of the solid-state structure of molecular materials has seen a considerable renaissance [1]. Polymorphism [2,3], crystal engineering [4,5], the rules governing packing tendencies [6], crystal packing calculations [7,8] and crystal structure prediction [9–11] have all been the subject of considerable investigation and in some cases controversy [12–14]. One of the key areas which governs success in the study of molecular materials, is an understanding of intermolecular interactions. The networks formed by conventional hydrogen bonds have been studied through pattern recognition [15]. The role of weak intermolecular interactions [16,17] and π–π stacking [18] in three dimensional structure formation has also been investigated. Previously, the crystal structure solution of flavanthrone (**1**) had been solved using a combination of powder diffraction and molecular modelling techniques [19] and an initial investigation into the intermolecular interactions of the crystal solid structure was made. The determination of the crystal structure was an extension to work done on determining the crystal structure of quinacridone [20] and the triphendioxazine pigments [21,22]. In this paper, we have revisited the structures of flavanthrone (**1**) [23] and indanthrone (**2**) [24], see Fig. 1, and with the benefit of hindsight from our recent study [25], employed crystal packing calculations to examine the important intermolecular interactions in the structures of both these molecules.

2. Experimental

The crystal structures of flavanthrone (**1**) and indanthrone (**2**) were taken from the Cambridge Crystallographic Database [26]. These structures were

* Corresponding author. Tel.: +44 161 721 1401; fax: +44 161 721 5240.
E-mail address: dthe@lubrizol-additives.com (D. Thetford).

0143-7208/$ - see front matter © 2004 Elsevier Ltd. All rights reserved.
doi:10.1016/j.dyepig.2004.11.002

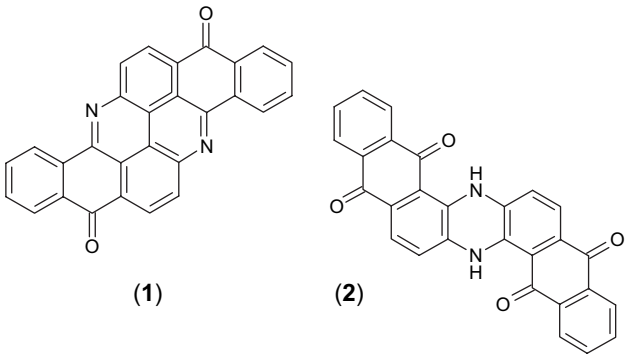

Fig. 1. The molecular structures of flavanthrone (**1**) and indanthrone (**2**).

determined some considerable time ago and consequently no hydrogen positions were reported. Hydrogens were fitted assuming standard bond lengths and angles. In indanthrone (**2**), this gives an intramolecular hydrogen bond of 1.84 Å which is consistent with the distances found for this intramolecular hydrogen bond in the Cambridge Database. A search for similar intramolecular hydrogen bonding fragments found 19 hits (mostly anthraquinones) and the minimum value found was 1.75 Å, the highest 2.11 Å and the mean 1.88 Å. The lengths and widths of the molecules are given in Table 1.

The molecular volume was calculated using CERIUS [27] and packing coefficients determined by considering the molecular volumes, the number of molecules in the cell and the unit cell volume. This is a measure of how efficient the molecules are at using space in the solid state. The basic crystallographic data for these molecules is summarised in Table 1.

Table 1
The basic crystallographic data for flavanthrone and indanthrone

Structural detail	Flavanthrone	Indanthrone
Refcode	FLAVAN	INDANT
a (Å)	27.92	30.83
b (Å)	3.80	3.833
c (Å)	8.10	7.845
α (°)	90.00	90.00
β (°)	95.00	91.92
γ (°)	90.00	90.00
Z	2	2
Space group	P21/a	P21/a
R-factor	0.16	0.13
Density (g cm^{-3})	1.58	1.58
Molecular volume (Å^3)	333.4	351.0
Cell volume (Å^3)	856.1	926.5
Packing coefficient	0.78	0.76
π–π stacking (Å)	3.47	3.40
Molecular length (Å)	15.7	17.99
Molecular width (Å)	8.1	5.4
Herringbone angle (°)	48.1	52.7

All the basic crystallographic data were taken from Refs. [23,24]. The other data were calculated as part of this work.

The lattice energies were determined for these molecules using the traditional approach. The basic equation for describing the lattice energy (E_{latt}) is shown in the equation below. The lattice energy can be calculated by summing all the atom–atom interactions between a central molecule containing *n* atoms and the *N* surrounding molecules each containing *n*′ atoms. The principles behind these calculations have been described elsewhere [8]. HABIT95 [28] was used in all the lattice energy calculations as it permits the important intermolecular interactions to be broken down both in particular crystallographic directions and onto particular atoms or groups. An important part of the lattice energy calculation is the electrostatic contribution. These are accounted for by atomic charges on each of the atoms in the molecule. In this study, these were determined using the AM1 Hamiltonian in the MOPAC program [29]. During either the molecular orbital calculations or crystal packing calculations, no minimization of the experimental structure was permitted.

$$E_{\text{latt}} = 1/2 \sum_{k=1}^{N} \sum_{i=1}^{n} \sum_{j=1}^{n'} \sum V_{kij}$$

3. Results and discussion

3.1. Lattice energies

The lattice energies for flavanthrone and indanthrone were calculated at various sizes of crystal ranging from 5 to 60 Å. This is shown in Fig. 2, both plots show the same basic profile, an initial increase is followed by the reaching of a plateau region. This reflects the distance dependence of the interatomic interaction potentials which are dependent on inverse powers of the interatomic distances. At large separation distances their contribution will be negligible [30]. In the case of

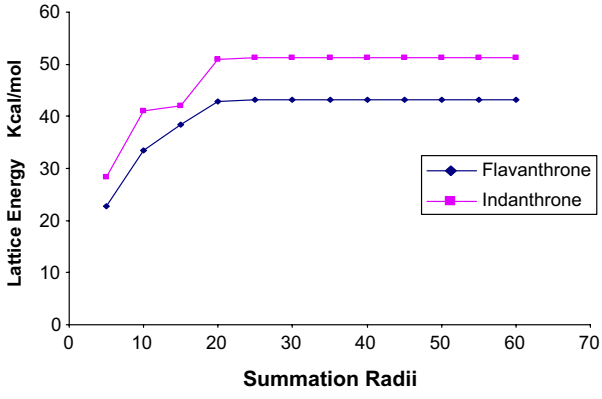

Fig. 2. The lattice energies of flavanthrone and indanthrone as a function of summation limit.

indanthrone, the number of intermolecular contacts varies from 2 at 5 Å to around 750 at 55 Å.

Overall, the lattice energy for flavanthrone was −43.3 kcal/mol and for indanthrone was −51.3 kcal/mol. The majority of the lattice energy comes from Van der Waals contributions. The electrostatic energy only plays a minor role in the overall lattice energy. The individual contributions are summarised in Table 2. These lattice energies are interesting as flavanthrone is a bigger molecule but has lower lattice energy. This reflects the important role of the additional functional groups in indanthrone (two extra C=O and N–H units).

3.2. Intermolecular interactions

The lattice energy can be broken down along specific crystallographic directions. For flavanthrone and indanthrone, these are shown in Tables 3 and 4, respectively. For flavanthrone the most important interaction is the π–π stacking (−11.2 kcal/mol) which runs up and down the *b*-axis. These interactions contribute around 52% of the lattice energy. The other interactions are down the *c*-axis (−3.2 kcal/mol) and along the *bc*-direction (−1.3 kcal/mol). Summed together these six interactions are worth around three quarters of the total lattice energy. All the subsequent interactions are worth less than 1 kcal/mol and so are not listed in Table 3. The interactions along the *c*-axis are a result of C–H:::::N dimer contacts at around 2.89 Å and those along *bc* are a result of the C–H:::::O interactions at 2.53 Å. The view down the *b*-axis (i.e in the *ac* plane) for flavanthrone is shown in Fig. 3.

The important intermolecular interactions are given for indanthrone in Table 4. The similarity in the packing between indanthrone and flavanthrone is clear from an inspection of Tables 3 and 4. The same *U*, *V*, *W* and *Z* values are present in both tables indicating a similar structure in the first coordination sphere around the central molecule. In indanthrone, the π–π interactions run along the *b*-axis with an interaction energy of −14.2 kcal/mol. This increased value is consistent with the closer π–π stacking distance observed in indanthrone (3.4 Å) compared to flavanthrone (3.47 Å). The important intermolecular interactions, those with a value greater than 1 kcal/mol, account for 75% of the total lattice energy. In indanthrone, the C–H:::::O interactions are slightly weaker than those for flavanthrone which is again consistent with the C–H:::::O distances of 2.45 Å in flavanthrone and 2.53 Å in indanthrone. In indanthrone, the C–H:::::O bonding is slightly more complicated than in flavanthrone with contacts forming dimers at 3.01 Å along the *c*-axis. This is supplemented by some electrostatic interactions at a slightly longer range between N–H:::::O=C groups. Additional C–H:::::O contacts at 2.53 Å are formed along the *bc* direction in a similar manner to flavanthrone. The view down the *b*-axis of indanthrone is shown in Fig. 4.

Table 2
The lattice energies for flavanthrone and indanthrone

	Flavanthrone	Indanthrone
Lattice energy	−43.26	−51.19
Attractive (VdW)	−71.83	−80.27
Repulsive (VdW)	28.47	29.77
Electrostatic	0.09	−0.70

Results in kcal/mol are quoted at 30 Å.

Table 3
The important intermolecular interactions in flavanthrone

U	*V*	*W*	*Z*	Energy	Description
0	1	0	1	−11.2	π–π
0	−1	0	1	−11.2	π–π
0	0	1	1	−3.2	C–H:::::N dimer at 2.89 Å
0	0	−1	1	−3.2	C–H:::::N dimer at 2.89 Å
0	1	1	1	−1.3	C–H:::::O at 2.45 Å
0	−1	−1	1	−1.3	C–H:::::O at 2.45 Å

The *U*, *V* and *W* values are the translations along *a*, *b* and *c*, respectively. *Z* is the number of the symmetry operation used to generate the molecule involved in the interaction. The origin of molecule in such a description is (*UVW*) 0,0,0 with *Z* = 1. Results in kcal/mol are quoted at 30Å.

3.3. Individual atomic contributions

The routines in HABIT95 [28] permit the breakdown of the lattice energy onto the atoms in a molecule. This breakdown can be very informative in identifying the role of different groups in the molecular unit to the crystal packing. In this section we will consider both the aromatic units making up the two structures and the role of smaller fragments such as carbonyl groups.

In both flavanthrone and indanthrone, the structures can be broken down into four constituent aromatic

Table 4
The important intermolecular interactions in indanthrone

U	*V*	*W*	*Z*	Energy	Description
0	1	0	1	−14.2	π–π
0	−1	0	1	−14.2	π–π
0	0	1	1	−2.6	C–H:::::O dimer at 3.01 Å
0	0	−1	1	−2.6	C–H:::::O dimer at 3.01 Å
0	1	1	1	−2.4	C–H:::::O at 2.53 Å
0	−1	−1	1	−2.4	C–H:::::O at 2.53 Å

The *U*, *V* and *W* values are the translations along *a*, *b* and *c*, respectively. *Z* is the number of the symmetry operation used to generate the molecule involved in the interaction. The origin of molecule in such a description is (*UVW*) 0,0,0 with *Z* = 1. Results in kcal/mol are quoted at 30 Å.

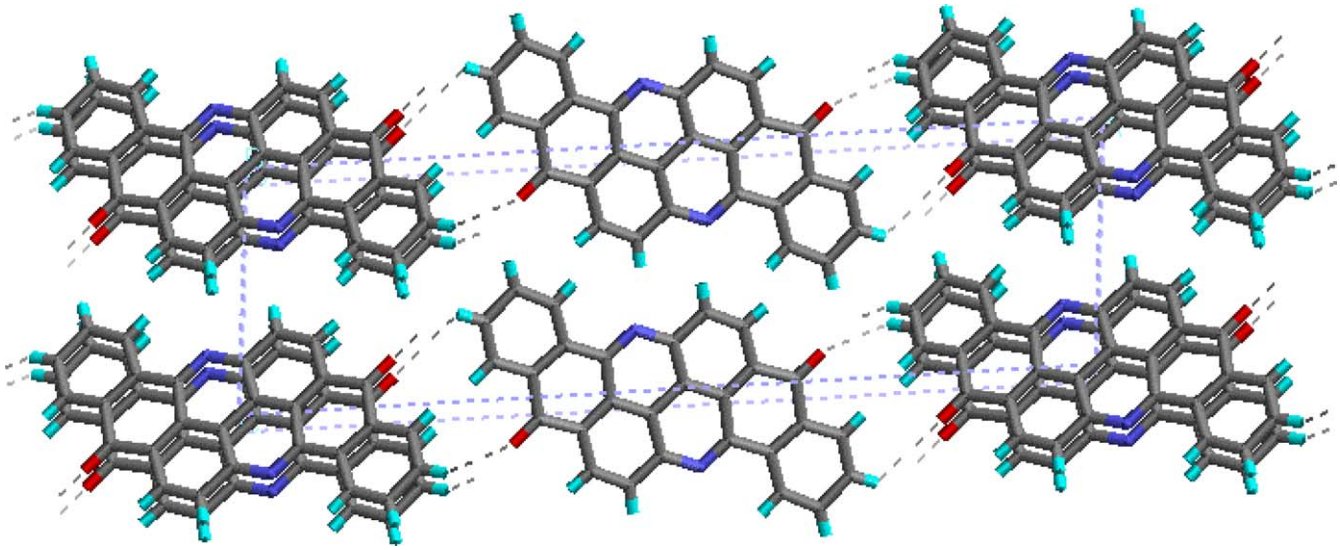

Fig. 3. The view of crystal packing in flavanthrone down the *b*-axis.

units. This is shown in Fig. 5 where these units are shown plus their respective contributions to the lattice energies. In Fig. 5, it is clear that the aromatic units on the ends of the molecules (structure unit 1) contribute roughly the same amount (8.7 kcal/mol) to the total lattice energy. The keto unit (structure unit 2) in flavanthrone and indanthone differ slightly in structure and this is reflected in their respective contributions (9 and 10.5 kcal/mol) to the total solid state energy. Perhaps the biggest difference is in the fourth structural unit where the contributions vary form 5.9 kcal/mol in flavanthrone to 9.6 kcal/mol in indanthrone. The difference in contributions from fragment 3 is due to the unit being between fragments of greater polarity in indanthrone than in flavanthrone.

In both flavanthrone and indanthrone, the contributions from the carbonyl units are the same at around an average value of 3.8 kcal/mol. It is interesting to note that in indanthrone there are two different carbonyl environments and they make different contributions to the lattice energy. The carbonyl unit involved in the intramolecular hydrogen bond contributes 3.7 kcal/mol which is 0.3 kcal/mol less than the contribution from the other 'free' carbonyl unit. The hydrogens involved in the C–H::::O interactions make a contribution of 0.9 and 1.0 kcal/mol to the lattice energy in flavanthrone and indanthrone.

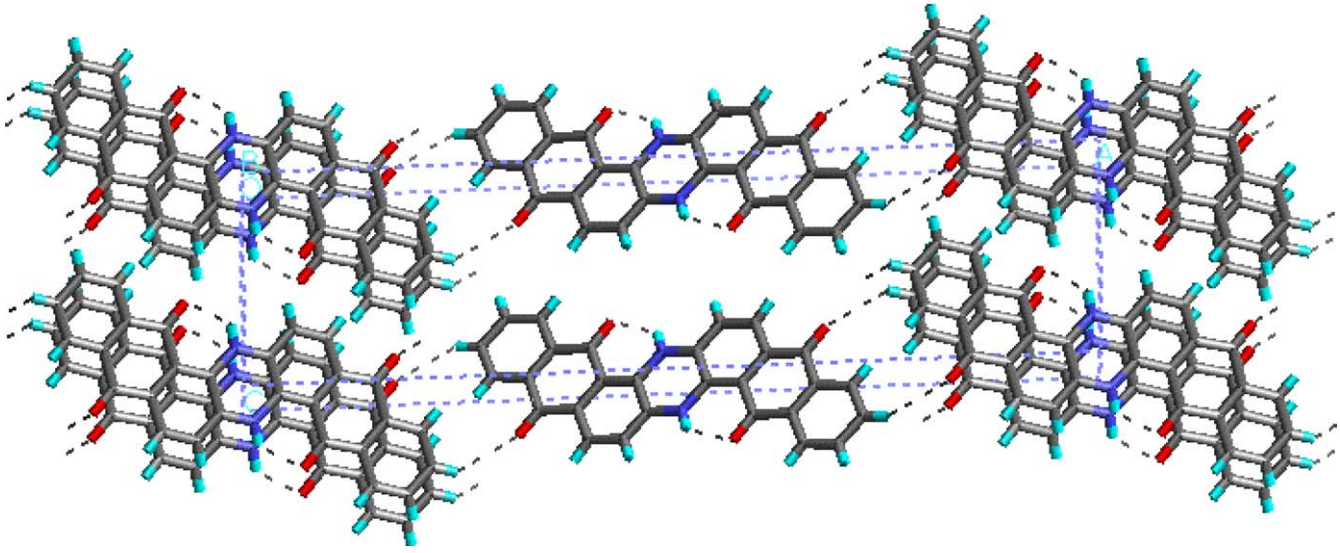

Fig. 4. The view of crystal packing in indanthrone down the *b*-axis.

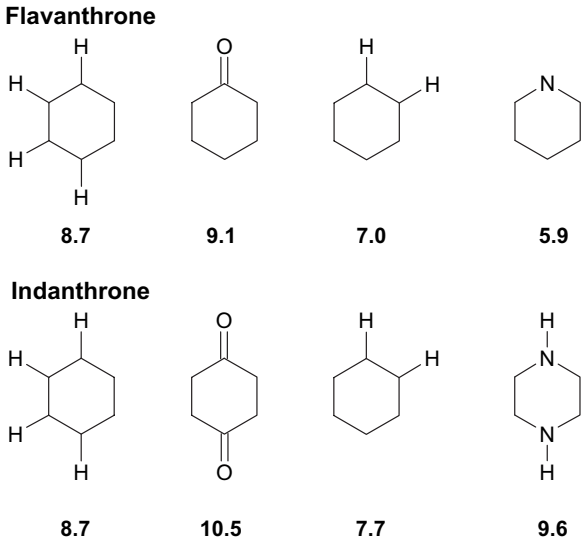

Fig. 5. The breakdown of the lattice energy into the constituent molecular fragments contribution for flavanthrone and indanthrone.

3.4. Weak hydrogen bond geometry in flavanthrone and indanthrone

One of the most interesting features of both these structures is the C–H::::O interaction patterns along the *bc* directions. The C–H::::O weak hydrogen bonds are formed at contact distances of 2.45 Å (flavanthrone) and 2.53 Å (indanthrone). The C=O::::H angles are 171 and 161°, respectively. The most interesting features are the geometry of the motif which is very similar in both cases. A single molecule forms four C–H::::O contacts (two C=O::::H and two C–H::::O). Since the molecules are symmetrical, we need only consider one-half of the molecule. Each half can form an interaction using its carbonyl function and a hydrogen atom as shown in Fig. 6. In both flavanthrone and indanthrone, it is the same hydrogen (relative to the carbonyl) that is used. The atoms forming the interactions are supplied by two different molecules which are part of a π–π stack. Fig. 3 shows the packing of a cluster of flavanthrone molecules. A dimer from the π–π stack is clearly visible in the centre of the picture and either side shows

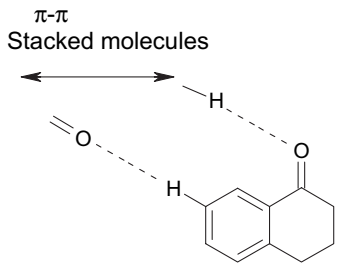

Fig. 6. Schematic showing the C–H::::O weak hydrogen bonding motif in flavanthrone and indanthrone.

Table 5
The basic structural features of C–H::::O bonding in flavanthrone, indanthrone and anthraquinone

Feature	Flavanthrone	Indanthrone	Anthraquinone
C–H::::O (Å)	2.45	2.53	2.65
C=O::::H angle (°)	171	161.4	161.6
Bite distance (Å)	4.78	4.90	4.75
Herringbone (°)	48.1	52.7	55.3

a flavanthrone molecule with the characteristic C–H::::O interactions biting across the dimer of the π–π stack.

This motif is not unique to flavanthrone and indanthrone and a similar arrangement is also observed for anthraquinone [31]. The data for this motif is summarised in Table 5. It should be noted that this motif is also observed in quinacridone [20] and indigo [32] where the C–H::::O weak hydrogen bonds are replaced with traditional hydrogen bonds. The correlation between the separation distance of these hydrogen bonding units, the π–π separation distance and herringbone angle are the subject of investigation.

4. Conclusions

Indanthrone (**2**) has lattice energy greater than that of flavanthrone (**1**). The majority of this difference seems to come from differences in π–π interactions. The π–π separation distance is smaller in indanthrone than in flavanthrone. One of the most interesting features is the similarity in the overall packing of these molecules. The first coordination sphere is identical in both systems and this cluster contributes 75% of the lattice energy. They both adopt similar herringbone packing motifs and their similarity is reflected in the breakdown of the important intermolecular interactions present in the structure. Weak hydrogen bonds such as C–H::::O interactions play an important role in completing the three dimensional packing with identical motifs being adopted by the two structures. The distance between the functional groups in these structures appears to be related to the herringbone angle in these structures. This particular aspect is the subject of further investigation.

References

[1] Erk P. Crystal design of high performance pigments. In: Smith HM, editor. High performance pigments. Weinheim: Wiley–VCH; 2002. p. 103–23. [chapter 8].
[2] Dunitz JD, Bernstein J. Acc Chem Res 1995;28(4):193–200.
[3] Gavezzotti A, Fillipini G. J Am Chem Soc 1995;117(49):12299–305.
[4] Desiraju GR. Crystal engineering – the design of organic solids. In: Materials science monographs, No. 54. Amsterdam: Elsevier; 1989.

[5] Aakeröy CB, Seddon KR. Chem Soc Rev 1993;22(6):397–407.
[6] Pratt Brock C, Dunitz JD. Chem Mater 1994;6(8):1118–27.
[7] Momany FA, Carruthers LM, McGuire RF, Scheraga HA. J Phys Chem 1974;78(16):1595–620.
[8] Charlton MH, Docherty R, Hutchings MG. J Chem Soc Perkin Trans 2 1995;2023–30.
[9] Karfunkel HR, Gdanitz RJ. J Comput Chem 1992;13(10):1171–83.
[10] Gavezzotti A. J Am Chem Soc 1991;113(12):4622–9.
[11] Holden JR, Du Z, Ammon HL. J Comput Chem 1993; 14(4):422–37.
[12] Maddox J. Nature 1988;335(6187):201.
[13] Cohen ML. Nature 1989;338(6213):291–2.
[14] Gavezzotti A. Acc Chem Res 1994;27(10):309–14.
[15] Etter MC. J Phys Chem 1991;95(12):4601–10.
[16] Desiraju GR, Sarma JARP. J Chem Soc Perkin Trans 2 1987; 1195.
[17] Desiraju GR. Acc Chem Res 2002;35(7):565–73.
[18] Hunter CA, Sanders JKM. J Am Chem Soc 1990;112(14):5525–34.
[19] Fagan PG. An examination of the crystal chemistry of some organic pigments using a combination of high resolution powder diffraction and computational chemistry techniques. PhD thesis, Strathclyde University, Dept. of Pure and Applied Chemistry; 1996. p. 122–35.
[20] Potts GD, Jones W, Bullock JF, Andrews SJ, Maginn SJ. J Chem Soc Chem Commun 1994;2565–6.
[21] Fagan PG, Roberts KJ, Docherty R, Chorlton AP, Potts GD, Jones W. Mol Cryst Liq Cryst 1994;248:277–89.
[22] Fagan PG, Hammond RB, Roberts KJ, Docherty R, Chorlton AP, Jones W, et al. Chem Mater 1995;7(12):2322–6.
[23] Stadler HP. Acta Cryst 1953;6:540–2.
[24] Bailey M. Acta Cryst 1955;8:182–5.
[25] Thetford D, Cherryman J, Chorlton AP, Docherty R. Dyes Pigments 2004;63(3):259–76.
[26] Allen FH, Kennard O, Taylor R. Acc Chem Res 1983;16(5):146–53.
[27] CERIUS 2 Version 1.6, Biosym/molecular simulations, 240/250 The Quorum, Barnwell Rd, Cambridge, UK; 1995.
[28] Docherty R, Clydesdale G, Roberts KJ. J Cryst Growth 1996; 166(1–4):78–83.
[29] Stewart JJP. J Comput Aided Mol Des 1990;4(1):1–105.
[30] Clydesdale G, Roberts KJ, Docherty R. Controlled particle, droplet and bubble formation. In: Wedlock D, editor. Butterworth-Heinemann; 1994. [chapter 4].
[31] Lenstra ATH, Van Loock JFJ. Bull Soc Chim Belg 1984; 93(12):1053–5.
[32] Potts GD. The Crystal chemistry of organic pigments. Phd thesis, Cambridge University; 1994.